Proceedings Paper:

Crack paths in plain and notched specimens of additively manufactured PLA under static loading

Adnan A. Ahmed and Luca Susmel

Department of Civil and Structural Engineering, The University of Sheffield, Mappin Street, Sheffield, S1 3JD, UK
aaahmed1@sheffield.ac.uk, https://orcid.org/0000-0002-6342-8878
l.susmel@sheffield.ac.uk, https://orcid.org/0000-0001-7753-9176

ABSTRACT. The aim of this paper is to investigate the way the infill angle affects, under static loading, the orientation of the crack paths in plain and notched additively manufactured polylactide (PLA). Un-notched specimens and samples containing a variety of geometrical features (i.e., notches) of 3D-printed PLA were fabricated horizontally by making the infill angle vary in the range 0°-90°. The generated experimental results demonstrate that, independently of the infill orientation, static breakage is the result of two different mechanisms, i.e., shear-stress-governed de-bonding between adjacent filaments and normal-stress-governed breakage of the filaments themselves. The combined effect of these two failure mechanisms results in the fact that the orientation of the crack paths fully depends on the orientation of the 3D-printed filaments.

KEYWORDS. Additive Manufacturing; PLA; Crack Paths.

INTRODUCTION

Thanks to its unique features, Additive Manufacturing (AM) is an innovative fabrication technology that can be used to fabricate, by joining materials layer upon layer, objects having complex shape, with this being done by reaching a remarkable level of accuracy in terms of both shape and dimensions.

Plastic materials (such as, for instance, acrylonitrile butadiene styrene, polylactide, polyphenyl sulfone, and polycarbonate) can be additively manufactured using powders, wires and flat sheets that are melted using different technologies.

Polylactide (PLA) is a biodegradable, absorbable and biocompatible polymer that can be 3D-printed by using low-cost commercial 3D-printers and it is daily used in situations of practical interest to fabricate a variety of components and objects. The mechanical properties of additively manufactured PLA are seen to be markedly influenced by a number of technological variables that include, amongst others: nozzle size, layer thickness, infill percentage, filling pattern, filling speed, and manufacturing temperature [1-4]. In this context, certainly the filling orientation is one of the most critical variables that affects the overall mechanical, strength, and fracture behaviour of additively manufactured plastics [5-8].

Owing to the important role AM is going to play in the near future, the aim of this investigation is to understand how the deposition angle affects both the static strength and the cracking behaviour of plain/notched objects made of additively manufactured PLA.

EXPERIMENTAL DETAILS

In order to investigate the orientation of the crack paths in plain and notched 3D-printed PLA subjected to static loading, a number of specimens were manufactured using as parent material white filaments of New Verbatim PLA with diameter equal to 2.85mm. The specimens employed in the present investigation were fabricated, via 3D-printer Ultimaker 2 Extended+, using the Fused Deposition Modelling (FDM) technology. The parameters for the 3D-printing process were set as follows: nozzle size equal to 0.4 mm, nozzle temperature to 240°C, build-plate temperature to 60°C, print speed to 30 mm/s, infill density to 100%, layer height to 0.1 mm, and shell thickness equal to 0.4 mm (i.e., equal to the nozzle diameter). All the specimens were fabricated flat on the build-plate (Fig. 1), with manufacturing angle θ_p varying from 0° to 90°. In the present investigation angle θ_p is defined as the angle between printing direction y_p and the longitudinal axis of the samples (Fig. 1). Both plain and notched specimens had thickness equal to 4 mm. The plain specimens had gross width equal to 25 mm and net width to 15 mm. The tensile samples containing two lateral notches had gross width equal to 25 mm, notch depth equal to 5 mm, and notch root radii, r_n, equal to 0.5 mm, 1 mm, and 3 mm. The bending specimens with single notch had gross width equal to 25 mm, notch depth equal to 10 mm, and notch root radii, r_n, equal to 0.4 mm, 0.5 mm, 1 mm, and 3 mm. Both the tensile and bending notched samples were fabricated with a notch opening angle equal to 0° as well as to 135° (open notches). The C(T) specimens were manufactured by setting the thickness equal to 20 mm and to 30 mm, with characteristic length B (defined according to ASTM D5045-14 [9]) equal to 20 mm and 30 mm, respectively. The un-notched specimens and the samples containing opposite notches were tested under tensile loading. The specimens with single lateral notches were tested under three point bending. The C(T) specimens were tested according to the experimental procedure being recommended by ASTM D5045-14 [9]. The static tests were run using a Shimadzu axial machine, with a displacement rate equal to 2 mm/sec. Three tests were run for any geometry/loading configuration being considered. All the tests were run up to the complete breakage of the samples. A detailed description of the experimental results considered in the present paper can be found in Ref. [8].
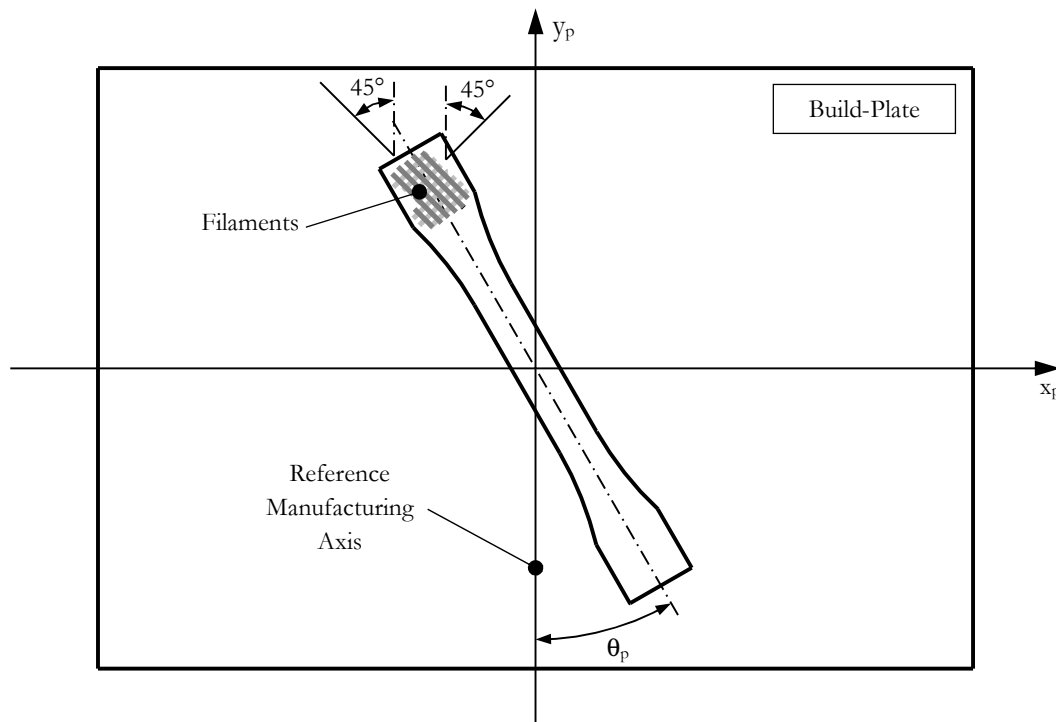

Figure 1: Definition of manufacturing angle θ_p.

STRESS VS. STRAIN BEHAVIOUR OF PLAIN PLA

The stress, σ, vs. strain, ε, diagrams reported in Figure 2 summarise the mechanical behaviour displayed under tensile loading by the AM material being investigated. These curves suggest that the relationship between stress and strain was

mainly linear up to the maximum stress recorded during testing, with this holding true independently of the value of the deposition angle, θ_p.

All the σ vs. ε curves generated by testing the plain specimens under tensile loading were re-analysed to derive Young's modulus, E, 0.2% proof stress, $\sigma_{0.2\%}$, and tensile strength, σ_{UTS}. The obtained results (see also Ref. [4]) are summarised in the diagrams of Fig. 3 where, for a shell thickness equal to 0.4 mm, the experimental values of E, $\sigma_{0.2\%}$, and σ_{UTS} are plotted against the infill angle, θ_p. These graphs show that the mechanical properties determined by making θ_p vary in the range 0°-90 ° fall all within an error interval of $\pm 2S_D$, with S_D being the standard deviation characterising the statistical dispersion of the mechanical properties being investigated. Therefore, according to the charts of Figure 3, it is possible to come to the conclusion that, for the specific 3D-printed material being investigated, the effect of θ_p on E, $\sigma_{0.2\%}$ and σ_{UTS} can be neglected with little loss of accuracy.
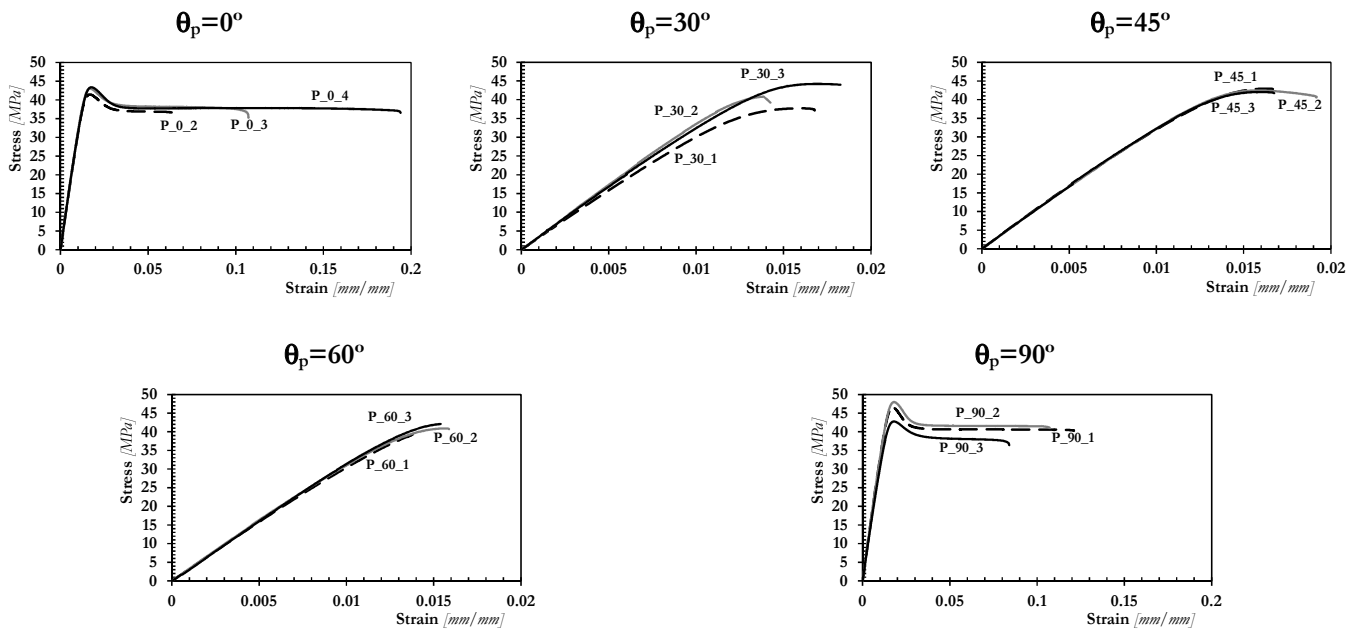

Figure 2: Stress-strain curves generated by testing the plain specimens [8].
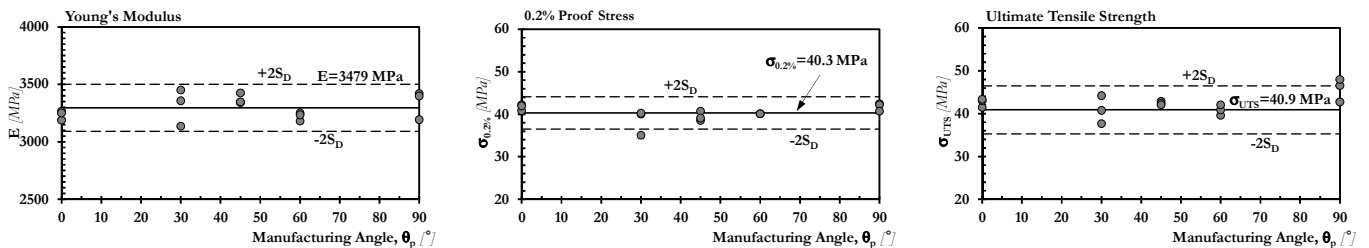

Figure 3: Young's modulus, 0.2% proof stress and ultimate tensile strength vs. manufacturing angle θ_p [8].

CRACK PATHS IN 3D-PRINTED PLA

In order to investigate the effect of the manufacturing angle, θ_p, on the orientation of the crack paths in 3D-printed PLA, initially attention was focused on the cracking behaviour displayed by the plain specimens. The matrix of failures reported in Figure 4 shows some of fracture surfaces that were observed in the un-notched samples loaded in tension during the initiation and the propagation phases. These pictures make it evident that, independently of the θ_p value, the cracks initiated on planes that were almost perpendicular to the direction of the tensile force. This initial phase, that was governed by the normal stress, resulted in meso-cracks having length of the order of the shell thickness (i.e., equal to about 0.4 mm). The following propagation process was seen to result in zig-zag crack paths following the directions of the 3D-printed filaments.

	$\theta_P=0°$	$\theta_P=30°$	$\theta_P=45°$	$\theta_P=60°$	$\theta_P=90°$
Initiation					
Propagation					
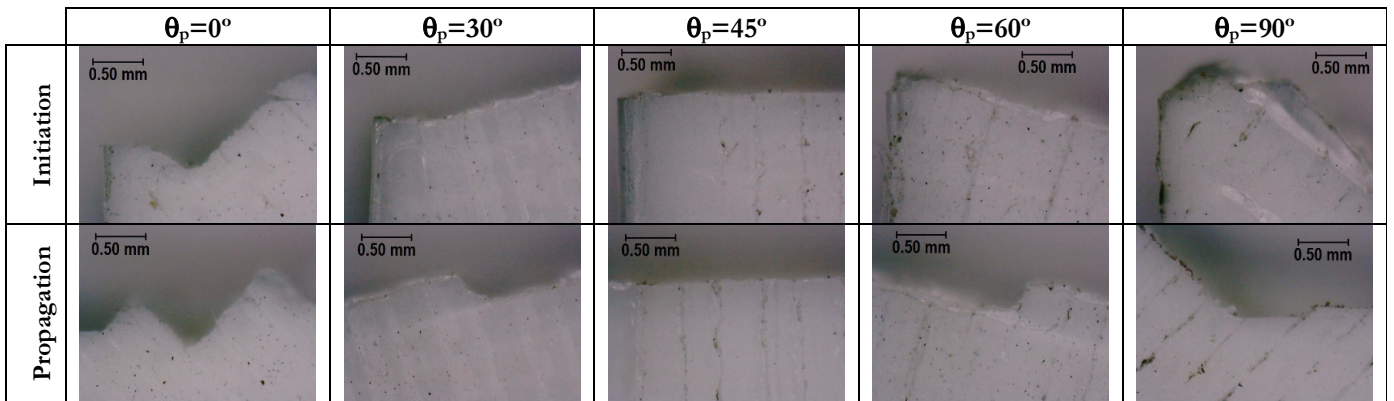
Figure 4: Crack paths in un-notched specimens of 3D-printed PLA under static tension [8].

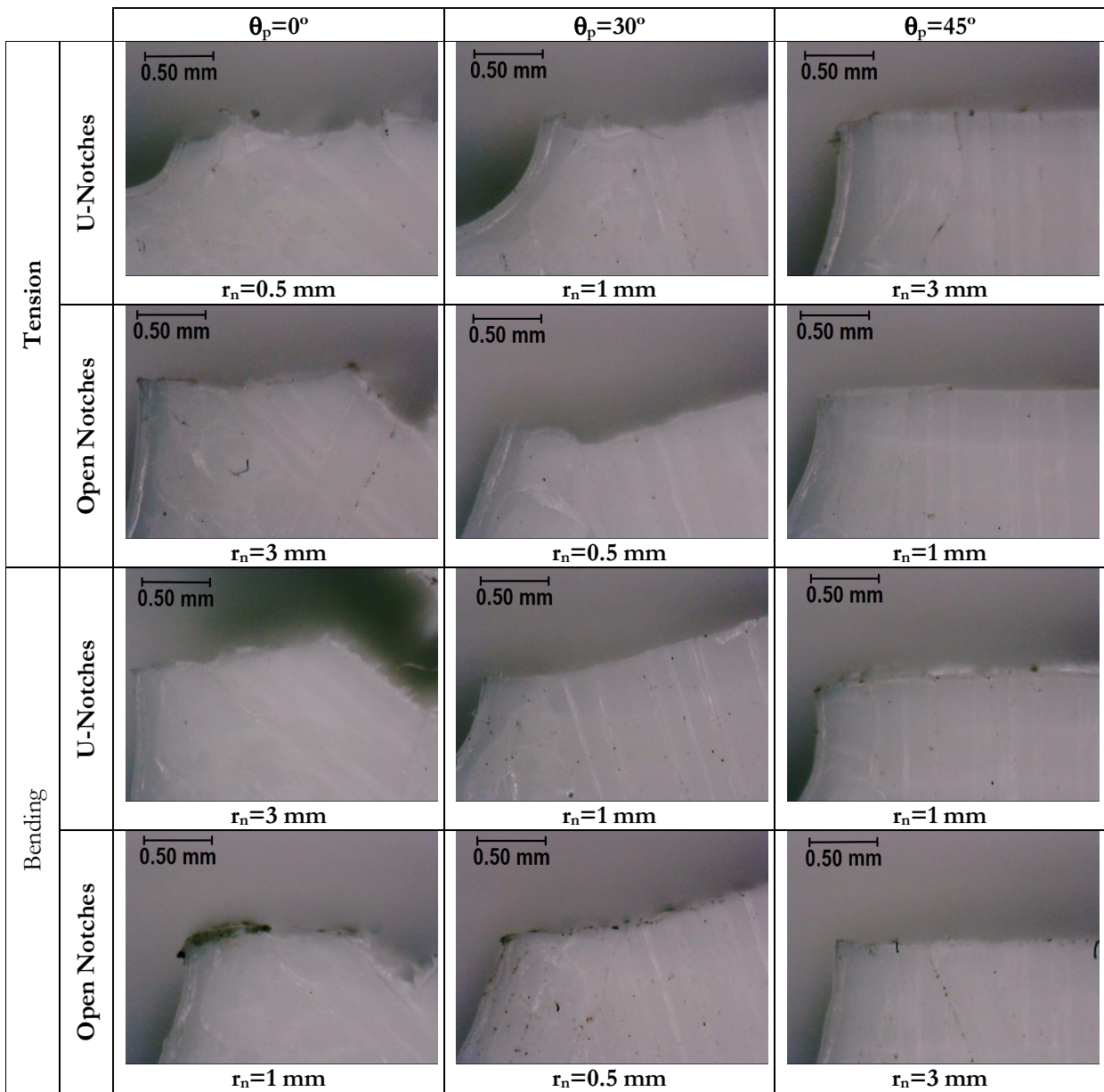|		$\theta_P=0°$	$\theta_P=30°$	$\theta_P=45°$
Tension	**U-Notches**	$r_n=0.5$ mm	$r_n=1$ mm	$r_n=3$ mm
	Open Notches	$r_n=3$ mm	$r_n=0.5$ mm	$r_n=1$ mm
Bending	**U-Notches**	$r_n=3$ mm	$r_n=1$ mm	$r_n=1$ mm
	Open Notches	$r_n=1$ mm	$r_n=0.5$ mm	$r_n=3$ mm

Figure 5: Crack paths in notched specimens of 3D-printed PLA under static tension as well as under static bending [8].

This rather complex cracking behaviour suggests that, irrespective of the filling direction, the propagation process was governed by two failure mechanisms, i.e., (i) de-bonding between adjacent filaments and (ii) rectilinear cracking of the filaments themselves.

Some examples showing the crack initiation regions in the notched specimens loaded in tension and in three-point bending are reported in Figure 5. Similar to the cracking behaviour observed in the un-notched samples (Fig. 4), the cracks were seen to initiate at the notch tips on those planes experiencing the maximum normal stress, with this holding true independently of type of loading, sharpness of the notch, and opening angle. These initial meso-cracks grew up to a distance from the notch tip equal to about the shell thickness (i.e., equal to about 0.4 mm). Subsequently, they kept propagating by following a zig-zag path, with the orientation of the crack paths being governed by the orientation of the 3D-printed filaments. This suggests that in the notched specimens as well the propagation phase was governed by a combined mechanism involving de-bonding and rectilinear cracking. It is important to observe here also that in some of the notched specimens, the cracks were seen to initiate on the flank of the notch, with this being the result of a defective adhesion, in the notch tip region, between the shell and the bulk material.
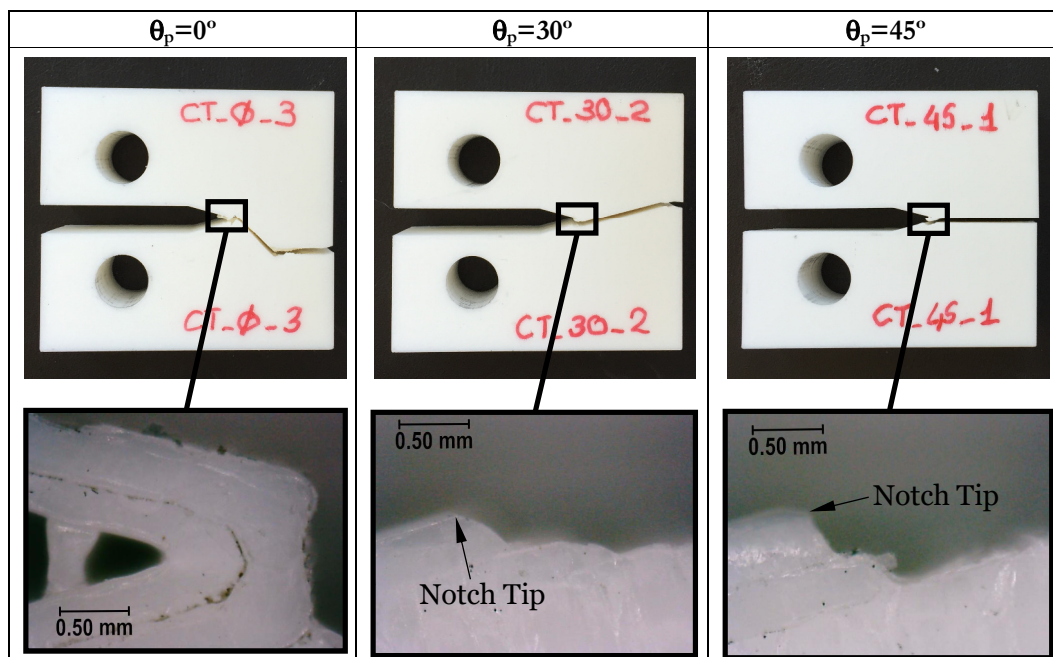

Figure 6: Crack paths in C(T) specimens of 3D-printed PLA with thickness equal to 20 mm [8].

Figure 6 shows some examples of the crack paths that were observed in the C(T) specimens with thickness equal to 20 mm. According to the pictures of Figure 6, in the C(T) specimens with thickness equal to both 20 mm and 30 mm the cracks were seen to propagate, at a macroscopic level, along the notch bisector, with this holding true independently from the value of manufacturing angle θ_P. In contrast, at a mesoscopic level, the crack propagation process was seen to be governed by local Mixed-Mode I/II mechanisms. Solely in the C(T) samples with $\theta_P=45°$ the cracking behaviour was seen to be governed by pure Mode I mechanisms also at a mesoscopic level. This can be explained by observing that a manufacturing angle, θ_P, equal to 45° led to 3D-printed filaments that were either parallel or perpendicular to the maximum Mode I direction. To conclude, it can be observed that, as shown in Figure 6, in the C(T) specimens the cracks were seen to initiate slightly away from the notch tip, with the initial propagation following the profile of the shell filament used to build the surface of the crack-like notches themselves.

CONCLUSIONS

The present paper describes the cracking behaviour that was observed in plain and notched specimens of 3D-printed PLA under both tensile loading and three-point bending. As per the specific 3D-printed PLA/manufacturing technology being considered in this investigation, the most relevant outcomes can be summarised as follows:

- independently of the value set for the manufacturing angle, θ_p, the mechanical behaviour of the investigated 3D-printed material can be model as linear-elastic up to final breakage;
- when θ_p varies in the range 0°-90°, Young's modulus, the 0.2% proof stress, and the material ultimate tensile strength are seen to be within two standard deviations of the mean;
- both in plain and notched specimens the crack initiation process occur on those planes experiencing the maximum mode I stress;
- the propagation phase (and, consequently, the orientation of the crack paths) depends on the orientation of the 3D-printed filaments;
- both in plain and notched specimens, and irrespective of the filling direction, the propagation is governed by two predominant failure mechanisms, i.e., (i) de-bonding between adjacent filaments and (ii) rectilinear cracking of the filaments themselves;
- for $\theta_p \neq 90°$, the crack propagation process at a mesoscopic level is governed by local Mixed-Mode I/II mechanisms;
- for $\theta_p = 90°$, the crack propagation process at a mesoscopic level is governed by local Mode I mechanisms.

REFERENCES

[1] de Ciurana, J., Serenó, L., Vallès, E., Selecting Process Parameters in RepRap Additive Manufacturing System for PLA Scaffolds Manufacture. Procedia CIRP 5 (2013) 152-157.

[2] Wittbrodt, B., Pearce, J. M., The effects of PLA color on material properties of 3-D printed components. Additive Manufacturing 8 (2015) 110-116.

[3] Fernandez-Vicente, M., Calle, W., Ferrandiz, S., Conejero, A., Effect of Infill Parameters on Tensile Mechanical Behavior in Desktop 3D Printing. 3D Printing and Additive Manufacturing 3 (2016) 183-192.

[4] Ezeh, O. H., Susmel, L., Designing additively manufacture notched PLA against static loading. In: Proceedings of International Symposium on Notch Fracture, Edited by S. Cicero et al., 29-31 March 2017, Santander, Spain, ISBN: 978-84-617-9611-3.

[5] Ahmed, A. A., Susmel, L., Additively manufactured PLA: strength and fracture behaviour under static loading. In: Proceedings of The BSSM's 12th International Conference on Advances in Experimental Mechanics, Sheffield, UK, 29-31 August, 2017 (available on-line at: http://www.bssm.org/2017papers).

[6] Ahmed, A. A., Susmel, L., Additively Manufactured PLA under static loading: strength/cracking behaviour vs. deposition angle. Procedia Structural Integrity 3 (2017) 498–507, 2017.

[7] Ahmed, A. A., Susmel, L., On the use of length scale parameters to assess the static strength of notched 3D-printed PLA. Frattura ed Integrità Strutturale 11/41 (2017) 252-259, 2017.

[8] Ahmed, A. A., Susmel, L. A material length scale based methodology to assess static strength of notched additively manufactured polylactide (PLA). Fatigue Fract Eng Mater Struct. (2018) 1–28 - https://doi.org/10.1111/ffe.12746

[9] ASTM D5045-14, Standard Test Methods for Plane-Strain Fracture Toughness and Strain Energy Release Rate of Plastic Materials, ASTM International, West Conshohocken, PA, 2014, www.astm.org.